Communications Physics

https://doi.org/10.1038/s42005-026-02601-y

Article in Press

# Dismantling complex networks based on higher-order graph neural network

Received: 26 February 2025

Accepted: 13 March 2026

Cite this article as: Zhou, W., Tan, S., Fang, Y. *et al.* Dismantling complex networks based on higher-order graph neural network. *Commun Phys* (2026). https://doi.org/10.1038/s42005-026-02601-y

Wennan Zhou, Suoyi Tan, Yang Fang, Xin Lü & Xiang Zhao

# Dismantling Complex Networks Based on Higher-order Graph Neural Network

**Wennan Zhou[1,+], Suoyi Tan[1,+], Yang Fang[1], Xin Lü[1,*], and Xiang Zhao[1,*]**

[1]College of Systems Engineering, National University of Defense Technology, Changsha, 410073, China
[*]These authors jointly supervised this work: xin.lu.lab@outlook.com, xiangzhao@nudt.edu.cn
[+]These authors contributed equally to this work: Wennan Zhou, Suoyi Tan

## ABSTRACT

Although existing research has confirmed the importance of higher-order structures in identifying key nodes within networks, the challenge remains on how to effectively integrate different types of higher-order information to precisely locate nodes that may be inconspicuous in lower-order structures but play a crucial role in higher-order interactions. To address this challenge, this paper proposes a general Higher-order Graph Neural Network representation learning framework (HoGNN) that can flexibly adapt to various types of higher-order relationships. Based on a robust theoretical framework, we develop a network dismantling model, SPR(Structural and Processual Role-aware Network Dismantling), which integrates multi-dimensional higher-order relations from both macro and micro perspectives. Empirical analysis demonstrated that the proposed model exhibits superior dismantling efficiency on both real-world and synthetic networks, using the minimal number of target node removals to collapse the network. Moreover, we show that SPR is more resilient to interference and accurately identifies key nodes in networks with multi-dimensional complex structures.



## Introduction

The exploration of complex systems spans across various domains, such as ecological[1], social[2], economic systems[3] and physical system[4]. These systems exhibit intricate characteristics, including non-linear behavior, self-organization, and diversity[3]. Representing systems as graphs provides deeper insights into their structure and dynamic features. Specifically, the robustness of networks serves as a critical measure of a system's ability to maintain performance under external pressures[5]. The problem of network dismantling, also known as the optimal percolation problem, aims to identify the minimum set of nodes (or edges) that can rapidly disrupt the network, causing the Giant Connected Component (GCC) or the Giant Connected Link (GCL) of the remaining network to decompose into isolated subcomponents, thereby effectively reducing the system's functionality[6](see Figure 1).

Network dismantling presents a widely applicable optimization problem, encompassing issues like optimal immunization (i.e., halting epidemic spread[7], controlling rumor propagation[8]), and combating criminal networks[9], etc. However, this presents an NP-hard challenge, meaning that even in small-scale networks, such optimization problems are computationally challenging[10]. Given the combinatorial optimization nature of network dismantling problems, numerous related mathematical planning models have been proposed[5]. However, due to computational complexity, these methods are not applicable to large-scale networks. Consequently, centrality-based methods have been proposed, including degree-based (degree centrality[11] and k-cores[12]), shortest path-based (closeness centrality[13] and betweenness centrality[14]), path-based (Katz centrality[15]), random walk-based (PageRank[16]), and non-backtracking random walk-based methods[17], among others. Research[18] has shown significant overlap between optimal solutions for decycling and dismantling, representative methods include the BPD algorithm (Belief Propagation-guided Decimation)[18], the Min-Sum algorithm[17] and the CoreHD method[19]. Additionally, researchers have expanded their focus to the problem of network dismantling under incomplete information[20]. With the rapid advancement in machine learning, novel paradigms have been introduced for network dismantling problems. For instance, GDM[6] introduces a new framework combining machine learning techniques to address network dismantling problems. FINDER[21] employs deep reinforcement learning algorithms to tackle these challenges. Wang et al[22,23] propose that the integration of deep graph neural networks demonstrate superior performance in network dismantling tasks, showcasing the potential of machine learning approaches. Furthermore, Artime et al[24] summarize these methods and provide a repository with ready-to-use scripts.

Previous research on network dismantling has primarily focused on systems with paired topologies, emphasizing the contribution of individual nodes to the overall network connectivity[25]. However, the selected Targeted Attack Node Set (TAS) often overlooks the role of nodes in their local clusters, resulting in the network retaining complex functional behaviors in many smaller sub-networks even after dismantling

operations. Local clusters and higher-order interactions complement each other, and existing research has confirmed that combining higher-order interactions helps identify the most important nodes[26]. Higher-order interactions are ubiquitous, referring to interactions involving no fewer than three nodes. These interaction cannot be decoupled into a linear combination of pairwise interactions[27]. For instance, in social systems, collaboration among multiple scholars to complete an academic paper is commonplace[28]. Binary relationships are insufficient to accurately describe the structural characteristics of such complex systems[29], with hypergraphs[28] and simplicial complexes[28] being the most common models for representing these complex structures. Simplicial complexes[30–34] and hypergraphs[35–40] capture higher-order relationships in networks in their unique ways: the former excels at showcasing hierarchical structures[40], while the latter performs exceptionally in handling combinations of nodes of arbitrary sizes[41]. However, most existing higher-order network representation learning models are restricted to specific network structures, limiting their generalizability and potentially overlooking the diverse higher-order interaction patterns coexisting in complex systems. Developing a unified higher-order network representation learning framework that can identify key nodes and analyze their roles across multiple levels of interaction is critical for understanding the structure and function of complex systems.

Here, we combine higher-order interactions to dismantle the network more thoroughly. Specifically, we propose a framework named SPR (Structural and Processual Role-aware Network Dismantling), which is shown in Figure 1, aimed at effectively capturing the overall characteristics of nodes in the network (referred to as structural roles) and individual characteristics of nodes (referred to as processual roles). To achieve this, we develop a Higher-order Graph Neural Network framework (HoGNN) that extends traditional graph convolution models, enabling efficient processing of higher-order network models such as hypergraphs and simplicial complexes. Specifically, we introduce a higher-order graph attention mechanism to dynamically capture the connections of each higher-order edge, thus generating more discriminative node embeddings. By integrating features from both structural and processual roles, we derive a final node dismantling score. Experimental results demonstrate that the proposed SPR framework outperforms existing methods on various real-world and synthetic networks. Moreover, we demonstrate that the dismantling method based on higher-order structural design exhibits greater adaptability, allowing for better identification of the functions of different substructures within the network and inflicting the most persistent impact on the network at minimal cost.

## Results

In this section, we provide a introduction to the SPR (Structural and Processual Role-aware Network Dismantling) model. We begin with an overview of the overall framework of the model, outlining the basic logical flow of SPR. Subsequently, we delve into a thorough analysis of each module of SPR using rigorous mathematical formulas. Finally, we present and discuss the experimental results.

### Components of the proposed SPR Framework

Figure 1 presents the comprehensive framework of the SPR model for identifying critical nodes in complex systems. The proposed methodology commences with the abstraction of real-world complex systems into graph representations, establishing a mathematical foundation for subsequent analysis. The SPR model subsequently processes the network's adjacency matrix $\mathscr{A} \in \mathbb{R}^{N\times N}$ as input, generating nodes dismantling scores vector as output through its four-stage computational architecture: (1) Feature engineering, (2) Macroscopic: Structural Role Encoding, (3) Microscopic: Processual Role Encoding, (4) Fusion and rank. This dual-perspective approach synergistically combines structural importance quantification from macroscopic topological properties with processual significance evaluation from microscopic interaction dynamics.

#### *Feature engineering*

For each network, the initial step involves generating a node embedding that preserves the original properties of the network, facilitating accurate advanced network analysis. To achieve a comprehensive understanding of node structure, we extracted a diverse set of features from both local and global perspectives. Local features included degree centrality and the average degree of neighbors, while global features encompassed the number of two-hop neighbors, local clustering coefficient, betweenness centrality, closeness centrality, and PageRank values. To establish an initial embedding matrix $X \in \mathbb{R}^{N\times 8}$, we incorporated a regulation constant to ensure a balanced representation of node characteristics.

#### *Macroscopic: Structural Role Encoding*

From a macro perspective, we regard the function of nodes in the overall network as structural roles. It is well known that in complex networks, the position of a node determines the different roles it plays in the process of network information propagation. Classic structural role classifications include authority nodes, boundary nodes, bridging nodes, etc. It is worth noting that two nodes that are far apart in a network may still perform similar roles in information propagation. For example, in academic networks, two leading scholars from different research fields might exert comparable levels of influence. Simply connecting nodes that share the same structural role, however, can overlook important nuances. Hy-

pergraphs, as a type of higher-order network model, offer a more effective means of capturing the intricate relationships between nodes and their distribution across different structural roles.

We employ the RolX algorithm for role extraction, a well-established method that factorizes the extracted structural feature matrix[42]. In the hypergraph, each extracted role is treated as a hyperedge, meaning that nodes with similar structural roles are grouped into the same hyperedge. The detailed process is outlined as follows.

**Structural Role Extraction** We employed the recursive feature extraction method outlined in the literature [43], which systematically aggregates local and neighborhood features to encapsulate global structural information. This approach facilitates the extraction of comprehensive role features, enhancing our analysis. Specifically, for each node, it first generates primary features by counting its adjacent edges and those within the node's egonet. Then, it recursively aggregates the primary features by applying simple aggregation operators, such as sum and mean, to the egonets. As the number of recursions increases, higher-order structural properties can be captured:

$$x_i^{(t+1)} = \left[ \sum_{j \in \mathcal{N}(i)} x_j^{(t)} || \sum_{j \in \mathcal{N}(i)} x_j^{(t)} / |\mathcal{N}(i)| \right], \tag{1}$$

$$X^R = \left[ X^{(1)} \parallel X^{(2)} \parallel \cdots \parallel X^{\top} \right], \tag{2}$$

where $X^R$ represents nodes' role embeddings, $T$ represents the number of iterations, $x_i^{(t)}$ represents the node feature of node $i$ at the $t$-th iteration. We then apply Non-negative Matrix Factorization (NMF) to generate a rank r approximation $JX_{SR-\varepsilon} \approx X^R$:

$$\underset{J, X_{SR-\varepsilon}}{\arg\min} \left\| X^R - JX_{SR-\varepsilon} \right\|_{fro} \text{s.t.} J \geq 0, X_{SR-\varepsilon} \geq 0, \tag{3}$$

where $\|\bullet\|_{fro}$ represents the Frobenius norm, the role number $r$ is determined by the minimum description length criterion, the role contribution matrix $J \in \mathbb{R}^{N \times M_{SR}}$ represents a node's membership in each role, node $v_i$ belongs to the $m$-th role if its $m$-th element is the maximum in its role embedding $J_i$. The role embedding matrix $X_{SR-\varepsilon} \in \mathbb{R}^{M_{SR} \times 2T}$ evaluates the contribution of each role to the estimated feature values. Due to the varied functions performed by each role in the network, attention mechanisms are employed to assign weights to these roles:

$$W_{SR-\varepsilon} = softmax(X_{SR-\varepsilon} B_1^{\top} + b_1), \tag{4}$$

where the resulting vector $W_{SR-\varepsilon} \in \mathbb{R}^{M_{SR} \times 1}$ is used to construct a diagonal matrix $\mathscr{W}_{SR-\varepsilon} = \text{diag}(W_{SR-\varepsilon}) \in \mathbb{R}^{M_{SR} \times M_{SR}}$ in subsequent operations.

**Learning Structural Role Score** According to the role contribution matrix $J \in \mathbb{R}^{N \times M_{SR}}$, the Structural Role-Node incidence matrix $\mathscr{H}_{SR}$ can be obtained. Subsequently, HoGNN operations (see Supplementary Note 2) are conducted to update vertex features, thereby obtaining feature embeddings:

$$X_{SR}^{(l+1)} = \sum_{k=0}^{K} \alpha_k T_k(\tilde{\mathscr{L}}_{SR}) X_{SR}^{(l)} \Theta, \tag{5}$$

where $T_k(\tilde{\mathscr{L}}_{SR}) = D_{SR-v}^{-1/2} \mathscr{H}_{SR} \mathscr{W}_{SR-\varepsilon} D_{SR-\varepsilon}^{-1} \mathscr{H}_{SR}^{\top} D_{SR-v}^{-1/2}$ represents the $k$-th order Chebyshev approximation of the scaled Laplacian, $D_{SR-v}$ and $D_{SR-\varepsilon}$ are the node degree matrix and hyperedge degree matrix obtained based on the Structural Role Node incidence matrix $\mathscr{H}_{SR}$, respectively. $X_{SR}^{(l+1)}$ and $X_{SR}^{(l)}$ represent the node features in the structural role encoding at layers $l$ and $l+1$, respectively.

#### *Microscopic: Processual Role Encoding*

From a micro perspective, individual nodes undergo role changes in different higher-order structures, referred to as processual roles. This perspective emphasizes the flexibility and contextual adaptability of nodes in the process of information dissemination. The processual role of a node is shaped not only by the broader network structure but also by its interactions with neighboring nodes. However, a node may simultaneously participate in multiple clusters of varying scales, assuming different roles within each. By examining the changes in node weights within simplicial complexes of different orders, we can uncover the subjective characteristics of nodes and understand how these dynamic shifts impact the overall network's efficiency and stability.

**Processual Role Extraction** Here we exemplify with the 2-dimensional simplicial complex. Firstly, from Supplementary Note 1, we obtain the incidence matrix $\mathscr{H}_{PR}$ of the 2-simplex. However, traditional pooling methods fail to discern the characteristic information of each node within the simplicial complex. Thus, by arranging and calculating the features of each node within the simplex, the function and contribution of each node within the simplex are determined, thereby constructing the simplex features through weighted aggregation:

$$X_{PR-\varepsilon} = \text{conv}\left(\text{MLP}(X_v) \cdot X_v, \quad \forall v \in \varepsilon_{PR}, \forall \varepsilon_{PR} \in \mathscr{E}_{PR}\right), \tag{6}$$

where $\mathscr{E}_{PR}$ denotes the set of all simplexes, and each simplex $\varepsilon_{PR}$ contains a subset of nodes $v$. The MLP transforms the raw node features into attention-like weights, which are then used to compute a weighted representation of the simplex.

Next, we introduce simplex attention generation. As nodes interact within the network, they aggregate information from their corresponding positions within the simplexes. When aggregating information from the simplexes, we recognize that the weights of adjacent simplexes of nodes differ. Hence, we incorporate the attention mechanism from Supplementary Note 2, where different weights are applied during node feature updates:

$$W_{PR-\varepsilon} = softmax(X_{PR-\varepsilon} B_2^{\top} + b_2). \tag{7}$$

where the resulting vector $W_{PR-\varepsilon} \in \mathbb{R}^{M_{PR}\times 1}$ is used to construct a diagonal matrix $\mathscr{W}_{PR-\varepsilon} = \mathrm{diag}(W_{PR-\varepsilon}) \in \mathbb{R}^{M_{PR}\times M_{PR}}$ in subsequent operations.

**Learning Processual Role Score** According to the Processual Role-Node incidence matrix $\mathscr{H}_{PR}$, HoGNN operations (see Supplementary Note 2) are conducted to update vertex features, thus obtaining updated feature embeddings:

$$X_{PR}^{(l+1)} = \sum_{k=0}^{K} \alpha_k T_k(\tilde{\mathscr{L}}_{PR}) X_{PR}^{(l)} \Theta, \tag{8}$$

where $T_k(\tilde{\mathscr{L}}_{PR}) = D_{PR-v}^{-1/2} \mathscr{H}_{PR} \mathscr{W}_{PR-\varepsilon} D_{PR-\varepsilon}^{-1} \mathscr{H}_{PR}^{\top} D_{PR-v}^{-1/2}$ represents the $k$-th order Chebyshev approximation of the scaled Laplacian, $D_{PR-v}$ and $D_{PR-\varepsilon}$ are the node degree matrix and simplex degree matrix obtained based on the Structural Role Node incidence matrix $\mathscr{H}_{PR}$, respectively. $X_{PR}^{(l+1)}$ and $X_{PR}^{(l)}$ represent the node features in the structural role encoding at layers $l$ and $l+1$, respectively. Finally, the node features of the 2-simplex, $X_{PR}^{2-\mathrm{sim}}$ can be obtained.

Similarly, we can obtain the node features of the 0-simplex and 1-simplex, $X_{PR}^{0-\mathrm{sim}}$ and $X_{PR}^{1-\mathrm{sim}}$. Node $i$ may simultaneously exist in multiple simplicial complexes of varying orders, and each order of simplicial complexes may contribute differently to the overall network function. For example, in 0-order complexes, the degree of a node may be an straightforward measure; whereas in higher-order complexes, the number of high-dimensional faces a node participates in, along with the connectivity of these faces, may be more significant. By introducing order weight factors, we capture the role diversity and influence distribution of nodes in the network's complex architecture in multiple dimensions, providing insights into specific simplices that play a central role in the network structure. Finally, the comprehensive weighted features of node $i$ across all orders of simplicial complexes is obtained through weighted summation:

$$X_{PR-i} = \sum_{f=0}^{q} W_{f-sim} \cdot X_{PR-i}^{f-\mathrm{sim}}, \tag{9}$$

where $X_{PR-i}$ is the total weighted features of node $i$, $X_{PR-i}^{f-\mathrm{sim}}$ is the base features of node $i$ in the $f$-order simplicial complex, and $W_{f-sim}$ is the order weight factor for the corresponding $j$-th order:

$$W_{f-\mathrm{sim}} = \frac{\exp(\mathrm{o}^{\top}\sigma(X_{PR}^{f-\mathrm{sim}} B_3^{\top} + b_3))}{\sum_{g=0}^{q} \exp(\mathrm{o}^{\top}\sigma(X_{PR}^{g-\mathrm{sim}} B_3^{\top} + b_3))}, \tag{10}$$

where $\mathrm{o} \in \mathbb{R}^q$ is the weight vector used to calculate attention scores.

#### *Fusion and Rank*

Here we have obtained the structural role features $X_{SR}$ and the processual role features $X_{PR}$ of the nodes. Next, we combine these two sets of features to obtain the dismantling score $S_i^{dis}$ for each node $i$:

$$S_i^{dis} = \sigma((X_{SR-i} \,\|\, X_{PR-i}) B_3^{\top} + b_3), \tag{11}$$

where $\sigma$ denotes the sigmoid function to normalize the scores $S_i^{dis} \in [0,1]$.

The dismantling score $S_i^{dis}$ represents the probability that node $v_i$ belongs to the target attack set $V_t$. Finally, based on the dismantling scores, the nodes with the highest scores are removed one by one, and the GCC is calculated after each removal until the GCC falls below a set threshold.

#### *Loss Function*

Our goal is to identify and remove nodes that have the greatest impact on the overall robustness of the network while minimizing the number of nodes removed[23]. Based on this, we construct the following loss function model:

$$\begin{aligned} L &\triangleq \mathbb{E}[|\text{Uninfluenced Nodes}|] + \gamma \mathbb{E}[|\text{TAS}|] \\ &= \sum_{v_i \in \mathscr{V}} \prod_{v_j \in \mathscr{N}(i)} \frac{1}{1 + s_j^{dis}} + \gamma \sum_{v_i \in \mathscr{V}} s_i^{dis}, \end{aligned} \tag{12}$$

where the weight factor $\gamma$ acts as a regulator, allowing us to balance flexibly between minimizing the number of nodes removed and maximizing the disruption of network structural integrity. Here, we set $\gamma = 1$.

## Experiment results

#### *Real-world networks*

**Overall performance comparison.** The dismantling performance of SPR on nine real-world networks is shown in Table 1, where the dismantling performance is measured by the Normalized Target Attack node Set size(NTAS, $\rho = |V_{TAS}|/|V_N|$). A smaller the value of $\rho$ indicates better dismantling performance. The last line in Table 1, "improv.%" represents the percentage improvement in the performance of our SPR model compared to the baseline model ($[\frac{\mathrm{value}_{\mathrm{sub-optimal}} - \mathrm{value}_{\mathrm{optimal}}}{\mathrm{value}_{\mathrm{sub-optimal}}}] \times 100$), with a positive value indicating an improvement in performance and a negative value indicates a decline in performance. As shown in Table 1, the SPR methods outperform state-of-the-art (SOTA) methods in most networks, especially in KKI, EconPoli, DNCEmails, and Crime. In higher-order structure-rich, high-clustering networks (e.g., NetScience, KKI), SPR effectively identifies key nodes embedded in nested structures, demonstrating superior performance. However, in the FilmTrust network, SPR slightly underperforms compared to GND. This is mainly due to the centralized nature of FilmTrust, where GND more rapidly identifies local hubs, achieving more efficient dismantling in the early stages. This suggests that in certain locally dominant networks, aggressive strategies may outperform global structure-aware approaches. All the experimental results reported in the main text are based on aggregating 2-order simplices (i.e., triangle structures). For results involving the aggregation of 0-order, 1-order, 3-order, and 4-order

simplices, please refer to Supplementary Note 6 for detailed data.

Figure 2 illustrates the performance of SPR on nine real-world networks. The results indicate that SPR consistently achieves more stable and uniform dismantling effects under various dismantling thresholds. Moreover, the area under the normalized GCC (NGCC) curve reflects the effectiveness of the dismantling scheme. As shown in Figure 2d, the area for SPR on the FilmTrust network is 0.029813, which is smaller than that of GND (0.030255). This suggests that our model focuses more on the global vulnerability of the network structure rather than localized "burst" effects, thereby more effectively disrupting network connectivity at the global level. In addition to node dismantling, we also evaluate the performance of SPR in the context of link removal. As shown in Supplementary Note 4.1 Table 2, SPR consistently outperforms other baseline methods across nine real-world networks in terms of link removal efficiency. We further evaluated the performance of the SPR model on large-scale datasets, with detailed results provided in Supplementary Note 8.

**The node removal sequences analysis.** Given the varying performance of different methods in dismantling the entire network, we conduct correlation analysis and visualize the degree distribution of attack nodes to further explore the differences in the node removal sequences generated by these methods. For each real-world network, node scores are first calculated using different dismantling methods to generate the removal order. Subsequently, the Kendall correlation coefficient between the node sequences obtained by different dismantling methods is calculated, with the results presented in Figure 3(a), (e), and (i) (See Supplementary Note 4 for more details). Across the nine real-world networks, the Kendall correlation coefficients between all methods are generally low, indicating significant deviations in the removal strategies of each method. In addition, the SPR method shows positive correlations with almost all baseline methods, indicating that top-ranked nodes are considered important by all methods. However, the lower Kendall correlation coefficient suggests that the dismantling results of SPR rely more heavily on its own methodological principles. In the visualization of attack node degree distribution, we selected two baseline algorithms with the best average performance-DCRS and NEES-for comparative analysis. The results are shown in Figure 3 (b-d), (f-h), and (j-l). It can be seen that the SPR algorithm can achieves effective network dismantling by selecting a minimal number of low-degree nodes. To intuitively demonstrate the importance of higher-order structural properties in network dismantling tasks, we selected the classic small-scale real-world network—Zachary's Karate Club network[2]—as a case study. Further detailed results are given in Supplementary Note 4.

**Explaining the SPR models**. Taking the DNCEmails dataset as a case study, we conduct an in-depth interpretability analysis of our model's predictions. Specifically, we systematically examine the topological characteristics of the attack node sets selected by different algorithms. For the SPR model, we track how key properties of the identified critical nodes evolve as the aggregated simplex order $f$ increases from 0 to 4. These properties include: node degree $<K>$, average degree of 1-hop neighbors $<1-K>$, average degree of 2-hop neighbors $2-<K>$, local clustering coefficient $<C>$, number of incident triangles $<T>$, tetrahedra $<Tr>$(3-simplices), and pentahedron $<P>$ (4-simplices). Results are summarized in Figure 4a. Furthermore, we compare SPR-2sim against several strong baselines (e.g., GND, CoreHD, FINDER) across these topological metrics, as shown in Figures 4c–Figures 4i. The comparisons highlight SPR's unique ability to prioritize nodes embedded in rich higher-order structures.

To further elucidate the internal mechanism, we also quantify the contribution weight of each simplex order to the final importance score during feature aggregation—see Figure 4b. Collectively, these results reveal that DNCEmails exhibits a highly intricate higher-order interaction structure. In such a dense communication network, SPR-3sim and SPR-4sim achieve dominant performance: their selected nodes participate in over 240 triangles and approximately 900 tetrahedra on average—substantially more than those chosen by other methods. A detailed interpretability analysis on other real-world datasets is provided in Supplementary Note 7.1.

### *Synthetic networks*

**Visualization results in typical synthetic network G.** In Figure 5, we present a typical network G enriched with higher-order information. This network consists of four star subgraphs and four complete subgraphs. Each star subgraph in one network corresponds to a complete subgraph in the other, with the hubs of these subgraphs fully connected. When a network contains a large number of fully connected subnetworks, both degree-based algorithms and machine learning-based algorithms tend to be misled by these structures. However, our proposed SPR method accurately identifies these structures and finds the optimal dismantling set.

**Comparison on different types of synthetic networks.** Figure 6(a) visually displays the average normalized TAS size $\rho$ across four synthetic networks. In this case, $\rho$ represents the average value over 20 instances of synthetic networks, each with $N = 1000$ nodes. We select eight of the most competitive and representative algorithms for comparison. As depicted in Figure 6, our SPR algorithm demonstrates strong competitiveness across all synthetic networks. Furthermore, we can observe that the robustness of node removal is related to the type of model network. The BA network appears to be the least robust due to its power-law degree distribution, where a small number of highly connected nodes dominate, while the WS network shows the highest robustness, given its more uniform connectivity structure.

To further explore the impact of network size and average node degree on dismantling effectiveness, we focuse on the ER network. By fixing the network size at $N = 1000$ and varying the average node degree from 3 to 6, and conversely, by fixing the average degree at $<k>=4$ and scaling the network

size $N$, we explored different scenarios. For each setting, 20 instances of the ER network are generated, and the results are averaged. The outcomes, depicted in Figure 6(b) and Figure 6(c), demonstrate that as network density increases, more attack nodes are required to achieve effective dismantling. Similarly, as the network size increases, the number of necessary attack nodes also rises. Despite these challenges, the SPR algorithm consistently accomplishes the dismantling task with high efficiency.

#### *Ablation study*

Our proposed Structural and Processual Role-aware Network Dismantling (SPR) framework calculates the dismantling score of nodes from two perspectives: the macro perspective of node structural role encoding and the micro perspective of node processual role encoding. To assess the individual impact of these two encoding strategies on overall performance, we introduced two variants of SPR: one without structural role encoding (SR) and the other without processual role encoding (PR), with the dismantling performance shown in Table 2. The results clearly indicate that removing either structural or processual role encoding leads to a decline in performance across all real-world networks. The full SPR model, which integrates both encoding strategies, consistently achieves the best results, demonstrating the complementary effectiveness of structural and processual role encoding in identifying critical nodes for network dismantling. We have also conducted sensitivity analysis of the key hyperparameters in our model, as detailed in Supplementary Note 9.

Further analysis reveals that in certain datasets (such as FilmTrust, RoviraVirgili, DNCEmails, Figeys, Crime, PPI, and NetScience), removing structural role encoding (w/o SR) has a particularly significant impact on model performance. In contrast, in other datasets (such as KKI and EconPoli), removing Processual role encoding (w/o PR) leads to a more severe performance decline. This difference highlights the fundamental distinction in the information propagation mechanisms across different types of networks. Specifically, in social networks (e.g., FilmTrust and RoviraVirgili) and communication networks (e.g., DNCEmails), the topological position of nodes (such as centrality, etc.) plays a decisive role in their influence within the network. These networks typically have higher average degrees and clustering coefficients, with tighter local connections. The structural roles of nodes largely determine their importance in network connectivity and stability. Therefore, in these scenarios, structural role encoding is particularly important. In contrast, in networks like EconPoli and KKI, the overall network is more sparse, with lower clustering coefficients and a lack of distinct local structural features between nodes. In such cases, the dynamic behavior of nodes is more reflective of their actual influence. Hence, for these networks, process role encoding plays a more critical role in capturing the dynamic behavior of nodes and their impact on the network.

## Discussion

Existing research has confirmed the significant role of higher-order structures on the architecture and functionality of networks. However, most current network dismantling methods are limited to simple topological networks, often overlooking these higher-order structures. In light of this, our study explores the critical role that higher-order network structures play in network dismantling. To address this, we propose HoGNN, a unified higher-order network representation learning framework capable of flexibly handling both simplicial complexes and hypergraphs. This framework dynamically evaluates and learns the connection weights of higher-order edges, generating highly discriminative node embeddings. Building upon HoGNN, we developed the SPR (Structural and Processual Role-aware Network Dismantling) model, which effectively captures the macro-architectural features of a network while accounting for the micro-interactions between nodes.

Our experimental results, derived from a range of real-world and synthetic networks, demonstrate that SPR consistently achieves superior dismantling performance. Specifically, the SPR framework's ability to model higher-order structures allows for a more comprehensive and accurate representation of real systems. This capability enables it to generate effective and targeted attack strategies for disrupting network structures, showing outstanding performance in networks rich in higher-order organizational structures.

While the current focus of SPR is on network dismantling, the underlying principles of the model-particularly its ability to learn discriminative node embeddings by integrating structural and dynamic roles-can potentially be extended to other network optimization tasks. For example, in network immunization [44], identifying the most influential nodes for vaccination is conceptually similar to dismantling, where the goal is to fragment the network by removing key nodes. Similarly, in influence maximization, selecting seed nodes that can maximize information spread could benefit from SPR's ability to identify structurally and functionally critical nodes. Moreover, in network control, where the aim is to identify a minimal set of nodes that can steer the system toward a desired state, SPR's higher-order representation learning may help uncover control hubs that are not apparent in simple graph models.

However, the current model still faces efficiency challenges when applied to extremely large-scale or dense networks. In future work, we plan to explore techniques such as graph coarsening, role clustering, and local approximation, aiming to maintain high identification accuracy while significantly improving scalability and computational efficiency-ultimately enabling fast and precise dismantling of ultra-large-scale networks.

## Methods

### Datasets

We assess the performance of SPR on both real-world and synthetic networks.

- Real-world networks consist of nine distinct application scenarios, each reflecting various topological characteristics, including FilmTrust[45], RoviraVigli[46], DNCEmails[47], PPI[48], Figeys[49], KKI[47], NetScience[47], Crime[47], and EconPoli[47]. Supplementary Note 3 offers a detailed introduction.
- Synthetic networks are generated using the NetworkX library[50], encompassing various network models, including ER (Erdös–Rényi) random networks, WS (Watts–Strogatz) small-world networks, BA (Barabási–Albert) scale-free networks, and PLC (Powerlaw-Cluster) networks. For each network type, 20 instances are randomly generated, and the average results are calculated for the final evaluation.

### Baselines

We compare our SPR algorithm with 20 baseline methods, which can be divided into three categories: node centrality-based methods, Heuristic-based approaches and machine learning-based methods. The node centrality-based methods include Degree Centrality (DC)[11], Betweenness Centrality (BC)[14], Closeness Centrality (CC)[13], Eigenvector Centrality (EC)[51], Harmonic Centrality (HC)[52], PageRank (PR)[16] and DomiRank Centrality (DR)[53]. The heuristic-based methods encompass Collective Influence (CI)[10], Vertex Entanglement (VE)[54] and Generalized Network Dismantling (GND)[55]. The machine learning-based methods encompass DeepWalk (DW)[56], Node2Vec (NV)[57], Role2Vec (RV)[58], Graph Convolutional Network (GCN)[59], Graph Attention Network (GAT)[60], FInding key players in Networks through DEep Reinforcement learning (FINDER)[21], Graph Dismantling with Machine learning (GDM)[6], Neural Extraction framework for multiscale Essential Structures (NEES)[61], Neural Influence Ranking Model (NIRM)[22], and Diffusion Competence and Role Significance (DCRS)[23]. Supplementary Note 3 provides descriptions of these baseline methods. In addition, we also conducted comparative experiments on dynamic dismantling, and the baseline method used and their experimental results are detailed in Supplementary Note 5.

It is important to note that, with the exception of NEES, NIRM, and DCRS, methods such as DW, NV, RV, GCN, and GAT are originally designed for network representation learning tasks. To adapt these methods for the ND task, we make specific adjustments. For GCN and GAT, we add a final linear layer that takes node embeddings as input and outputs scores. Similarly, for DW, NV, and RV, we train separate Multi-Layer Perceptrons (MLPs) to map node embeddings to scores. These modifications are made to align the evaluation with the objective function of our SPR model, ensuring consistency across all methods.

## Data availability

All datasets supporting the findings of this study are available at the following GitHub repository: https://github.com/zhouwn/spr.

## Code availability

The custom code that supports the findings of this study is available at the following GitHub repository: https://github.com/zhouwn/spr.

## References


1. Mazzolini, A., Gherardi, M., Caselle, M., Cosentino Lagomarsino, M. & Osella, M. Statistics of shared components in complex component systems. *Phys. Rev. X* **8**, 021023 (2018).
2. Zachary, W. W. An information flow model for conflict and fission in small groups. *J. anthropological research* **33**, 452–473 (1977).
3. Grilli, J., Barabás, G., Michalska-Smith, M. J. & Allesina, S. Higher-order interactions stabilize dynamics in competitive network models. *Nature* **548**, 210–213 (2017).
4. Agrawal, S., Galmarini, S. & Kröger, M. Energy formulation for infinite structures: Order parameter for percolation, critical bonds, and power-law scaling of contact-based transport. *Phys. Rev. Lett.* **132**, 196101 (2024).
5. Krause, S. M., Danziger, M. M. & Zlatić, V. Hidden connectivity in networks with vulnerable classes of nodes. *Phys. Rev. X* **6**, 041022 (2016).
6. Grassia, M., De Domenico, M. & Mangioni, G. Machine learning dismantling and early-warning signals of disintegration in complex systems. *Nat. communications* **12**, 5190 (2021).
7. Osat, S., Papadopoulos, F., Teixeira, A. S. & Radicchi, F. Embedding-aided network dismantling. *Phys. Rev. Res.* **5**, 013076 (2023).
8. Cohen, R., Erez, K., Ben-Avraham, D. & Havlin, S. Breakdown of the internet under intentional attack. *Phys. review letters* **86**, 3682 (2001).
9. Musciotto, F. & Micciché, S. Effective strategies for targeted attacks to the network of cosa nostra affiliates. *EPJ Data Sci.* **11**, 11 (2022).
10. Morone, F., Min, B., Bo, L., Mari, R. & Makse, H. A. Collective influence algorithm to find influencers via optimal percolation in massively large social media. *Sci. reports* **6**, 30062 (2016).

**11.** Albert, R., Jeong, H. & Barabási, A.-L. Error and attack tolerance of complex networks. *nature* **406**, 378–382 (2000).

**12.** Wandelt, S., Sun, X., Feng, D., Zanin, M. & Havlin, S. A comparative analysis of approaches to network-dismantling. *Sci. reports* **8**, 13513 (2018).

**13.** Bonacich, P. Communication patterns in task-oriented groups. *Am. Sociol. Rev.* **62**, 1170–1182 (1987).

**14.** Freeman, L. C. A set of measures of centrality based on betweenness. *Sociometry* 35–41 (1977).

**15.** Newman, M. *Networks* (Oxford university press, 2018).

**16.** Page, L., Brin, S., Motwani, R., Winograd, T. *et al.* The pagerank citation ranking: Bringing order to the web. (1999).

**17.** Braunstein, A., Dall'Asta, L., Semerjian, G. & Zdeborová, L. Network dismantling. *Proc. Natl. Acad. Sci.* **113**, 12368–12373 (2016).

**18.** Mugisha, S. & Zhou, H.-J. Identifying optimal targets of network attack by belief propagation. *Phys. Rev. E* **94**, 012305 (2016).

**19.** Zdeborová, L., Zhang, P. & Zhou, H.-J. Fast and simple decycling and dismantling of networks. *Sci. reports* **6**, 37954 (2016).

**20.** Tan, S.-Y., Wu, J., Lü, L., Li, M.-J. & Lu, X. Efficient network disintegration under incomplete information: the comic effect of link prediction. *Sci. reports* **6**, 22916 (2016).

**21.** Fan, C., Zeng, L., Sun, Y. & Liu, Y.-Y. Finding key players in complex networks through deep reinforcement learning. *Nat. machine intelligence* **2**, 317–324 (2020).

**22.** Zhang, J. & Wang, B. Dismantling complex networks by a neural model trained from tiny networks. In *Proceedings of the 31st ACM International Conference on Information & Knowledge Management*, 2559–2568 (2022).

**23.** Zhang, J. & Wang, B. Encoding node diffusion competence and role significance for network dismantling. In *Proceedings of the ACM Web Conference 2023*, 111–121 (2023).

**24.** Artime, O. *et al.* Robustness and resilience of complex networks. *Nat. Rev. Phys.* **6**, 114–131 (2024).

**25.** Zügner, D., Akbarnejad, A. & Günnemann, S. Adversarial attacks on neural networks for graph data. In *Proceedings of the 24th ACM SIGKDD international conference on knowledge discovery & data mining*, 2847–2856 (2018).

**26.** Zeng, Y., Huang, Y., Ren, X.-L. & Lü, L. Identifying vital nodes through augmented random walks on higher-order networks. *Inf. Sci.* **679**, 121067 (2024).

**27.** Benson, A. R., Gleich, D. F. & Leskovec, J. Higher-order organization of complex networks. *Science* **353**, 163–166 (2016).

**28.** Torres, L., Blevins, A. S., Bassett, D. & Eliassi-Rad, T. The why, how, and when of representations for complex systems. *SIAM Rev.* **63**, 435–485 (2021).

**29.** Papillon, M., Sanborn, S., Hajij, M. & Miolane, N. Architectures of topological deep learning: A survey of message-passing topological neural networks. *arXiv preprint arXiv:2304.10031* (2023).

**30.** Ebli, S., Defferrard, M. & Spreemann, G. Simplicial neural networks. *arXiv preprint arXiv:2010.03633* (2020).

**31.** Yang, M., Isufi, E. & Leus, G. Simplicial convolutional neural networks. In *ICASSP 2022-2022 IEEE International Conference on Acoustics, Speech and Signal Processing (ICASSP)*, 8847–8851 (IEEE, 2022).

**32.** Bodnar, C. *et al.* Weisfeiler and lehman go topological: Message passing simplicial networks. In *International Conference on Machine Learning*, 1026–1037 (PMLR, 2021).

**33.** Chen, Y., Gel, Y. R. & Poor, H. V. Bscnets: Block simplicial complex neural networks. In *Proceedings of the aaai conference on artificial intelligence*, vol. 36, 6333–6341 (2022).

**34.** Hacker, C. k-simplex2vec: a simplicial extension of node2vec. *arXiv preprint arXiv:2010.05636* (2020).

**35.** Feng, Y., You, H., Zhang, Z., Ji, R. & Gao, Y. Hypergraph neural networks. In *Proceedings of the AAAI conference on artificial intelligence*, vol. 33, 3558–3565 (2019).

**36.** Jiang, J., Wei, Y., Feng, Y., Cao, J. & Gao, Y. Dynamic hypergraph neural networks. In *IJCAI*, 2635–2641 (2019).

**37.** Yadati, N. *et al.* Hypergcn: A new method for training graph convolutional networks on hypergraphs. *Adv. neural information processing systems* **32** (2019).

**38.** Huang, J. & Yang, J. Unignn: a unified framework for graph and hypergraph neural networks. *arXiv preprint arXiv:2105.00956* (2021).

**39.** Bai, S., Zhang, F. & Torr, P. H. Hypergraph convolution and hypergraph attention. *Pattern Recognit.* **110**, 107637 (2021).

**40.** Wu, H., Yan, Y. & Ng, M. K.-P. Hypergraph collaborative network on vertices and hyperedges. *IEEE Transactions on Pattern Analysis Mach. Intell.* **45**, 3245–3258 (2022).

**41.** Roddenberry, T. M., Glaze, N. & Segarra, S. Principled simplicial neural networks for trajectory prediction. In *International Conference on Machine Learning*, 9020–9029 (PMLR, 2021).

**42.** Henderson, K. *et al.* Rolx: structural role extraction & mining in large graphs. In *Proceedings of the 18th ACM SIGKDD international conference on Knowledge discovery and data mining*, 1231–1239 (2012).

**43.** Henderson, K. *et al.* It's who you know: graph mining using recursive structural features. In *Proceedings*

*of the 17th ACM SIGKDD international conference on Knowledge discovery and data mining*, 663–671 (2011).

**44.** Gu, W., Yang, C., Li, L., Hou, J. & Radicchi, F. Deep-learning-aided dismantling of interdependent networks. *Nat. Mach. Intell.* 1–12 (2025).

**45.** Guo, G., Zhang, J. & Yorke-Smith, N. A novel evidence-based bayesian similarity measure for recommender systems. *ACM Transactions on Web (TWEB)* **10**, 1–30 (2016).

**46.** Guimera, R., Danon, L., Diaz-Guilera, A., Giralt, F. & Arenas, A. Self-similar community structure in a network of human interactions. *Phys. review E* **68**, 065103 (2003).

**47.** Kunegis, J. Konect: the koblenz network collection. In *Proceedings of the 22nd international conference on world wide web*, 1343–1350 (2013).

**48.** Bu, D. *et al.* Topological structure analysis of the protein–protein interaction network in budding yeast. *Nucleic acids research* **31**, 2443–2450 (2003).

**49.** Ewing, R. M. *et al.* Large-scale mapping of human protein–protein interactions by mass spectrometry. *Mol. systems biology* **3**, 89 (2007).

**50.** Hagberg, A., Swart, P. J. & Schult, D. A. Exploring network structure, dynamics, and function using networkx. Tech. Rep., Los Alamos National Laboratory (LANL), Los Alamos, NM (United States) (2008).

**51.** Bonacich, P. Power and centrality: A family of measures. *Am. journal sociology* **92**, 1170–1182 (1987).

**52.** Boldi, P. & Vigna, S. Axioms for centrality. *Internet Math.* **10**, 222–262 (2014).

**53.** Engsig, M., Tejedor, A., Moreno, Y., Foufoula-Georgiou, E. & Kasmi, C. Domirank centrality reveals structural fragility of complex networks via node dominance. *Nat. communications* **15**, 56 (2024).

**54.** Huang, Y., Wang, H., Ren, X.-L. & Lü, L. Identifying key players in complex networks via network entanglement. *Commun. Phys.* **7**, 19 (2024).

**55.** Ren, X.-L., Gleinig, N., Helbing, D. & Antulov-Fantulin, N. Generalized network dismantling. *Proc. national academy sciences* **116**, 6554–6559 (2019).

**56.** Perozzi, B., Al-Rfou, R. & Skiena, S. Deepwalk: Online learning of social representations. In *Proceedings of the 20th ACM SIGKDD international conference on Knowledge discovery and data mining*, 701–710 (2014).

**57.** Grover, A. & Leskovec, J. node2vec: Scalable feature learning for networks. In *Proceedings of the 22nd ACM SIGKDD international conference on Knowledge discovery and data mining*, 855–864 (2016).

**58.** Ahmed, N. K. *et al.* Role-based graph embeddings. *IEEE Transactions on Knowl. Data Eng.* **34**, 2401–2415 (2020).

**59.** Kipf, T. N. & Welling, M. Semi-supervised classification with graph convolutional networks. *arXiv preprint arXiv:1609.02907* (2016).

**60.** Velickovic, P. *et al.* Graph attention networks. *stat* **1050**, 10–48550 (2017).

**61.** Liu, Q. & Wang, B. Neural extraction of multiscale essential structure for network dismantling. *Neural Networks* **154**, 99–108 (2022).

## Acknowledgements

The authors are grateful for the support from the National Key R&D Program of China (2022YFB3102600), National Natural Science Foundation of China (U25B2047, 62272469, 72474223, 62306322, 72025405, 72421002, 92467302, 72301285), Science and Technology Innovation Program of Hunan Province (2023RC1007, 2024RC3133, 2023JJ40685), the Innovation Research Foundation of National University of Defense Technology (JS24-04), the National Science and Technology Major Project for Brain Science and Brain-like Intelligence Technology (2025ZD0215700), the Major Program of Xiangjiang Laboratory (24XJJCYJ01001) and the Postgraduate Innovation Program of National University of Defense Technology (XJQY2024064). The authors thank Stefano Boccaletti for useful discussions.

## Author contributions statement

Idea and Supervise: Wennan Zhou, Suoyi Tan, Yang Fang, and Xiang Zhao. Data Analysis: Wennan Zhou, Suoyi Tan, Yang Fang, and Xiang Zhao. Writing Original Draft: Wennan Zhou, Suoyi Tan, and Yang Fang. Writing Discussions & Editing: Wennan Zhou, Suoyi Tan, Yang Fang, Xin Lü, Xiang Zhao.

## Competing interests

The authors declare no competing interests.

## Additional information

**Supplementary information** are also uploaded in the paper submission system.
**Correspondence** and requests for materials should be addressed to Xin Lü or Xiang Zhao.
**Accession codes** supporting the results of this study will be available at the GitHub repository after the paper is published.

## Figure legends

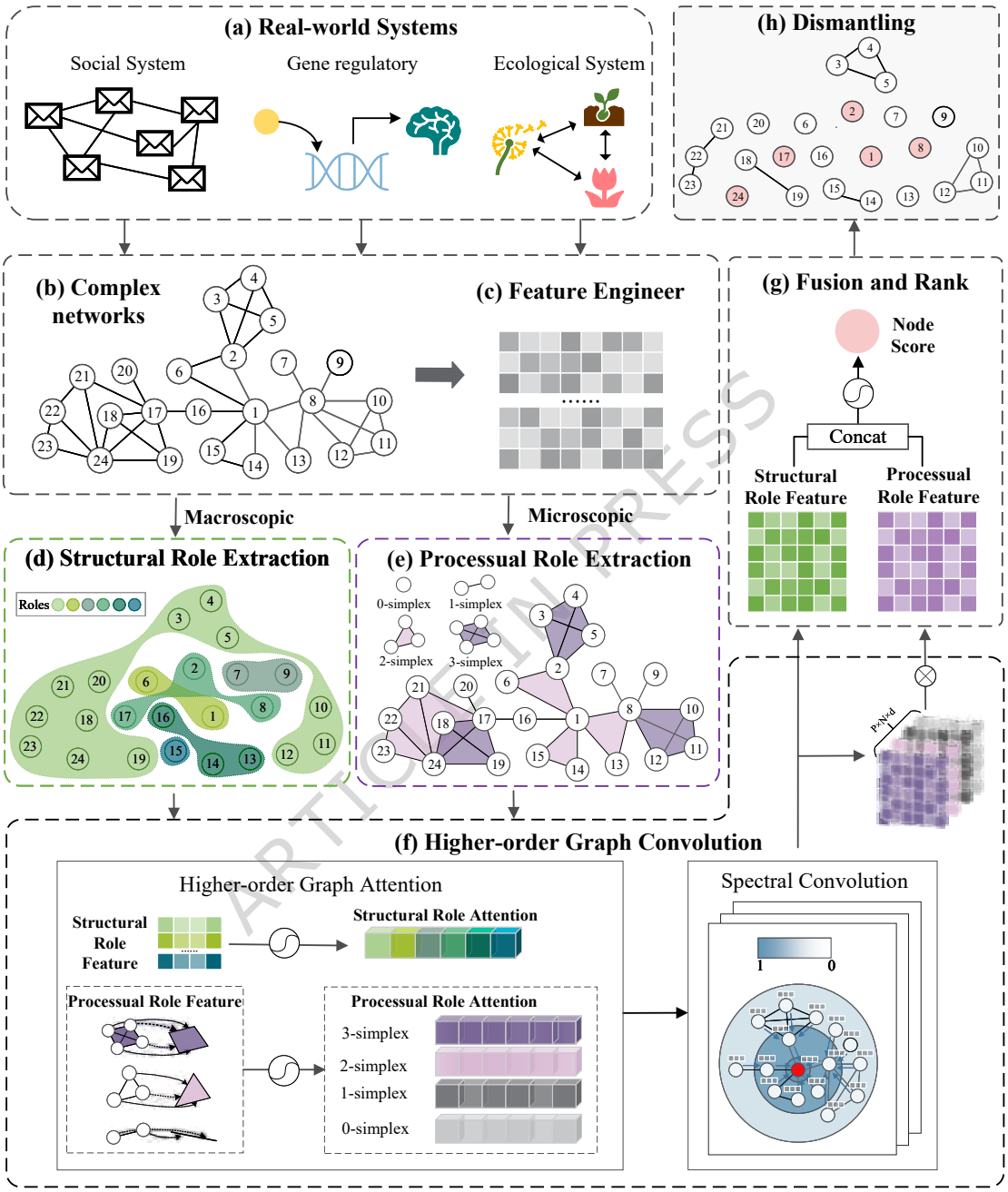


**Figure 1. Illustration of the proposed Structural and Processual Role-aware Network Dismantling (SPR) framework. It includes the following parts:** (a) Input a real-world system, (b) Abstracting it as a topological network, (c) Extract multidimensional features from the network from eight perspectives (e.g., degree centrality, clustering coefficient etc.), (d) Extract the structural roles of nodes from a macro perspective, (e) Extract the processual roles of nodes from a micro perspective, (f) Update the node features of both perspectives through Higher-order Graph Neural Network representation learning framework (HoGNN), which include two steps: graph attention mechanism and graph spectral convolution, (g) Combine the scores of nodes from both perspectives to obtain the final node scores, and (h) Select the nodes that need to be dismantled, where empty dots represent unselected nodes and pink dots represent targeted attack nodes, and remove the edges associated with them.

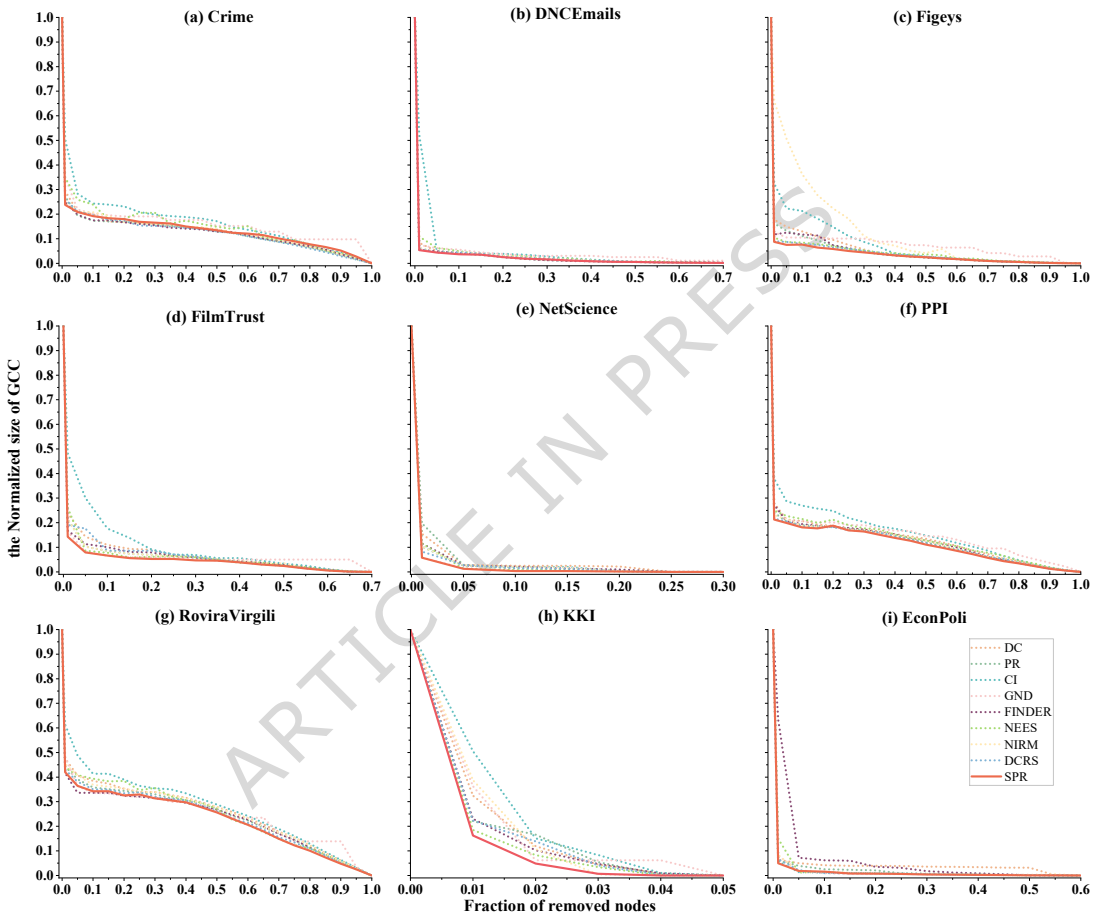


**Figure 2. Performance of SPR on nine real-world networks**. The evolution of the relative size of the largest connected component (robustness) whilst undergoing sequential node removal according to descending scores computed by various dismantling algorithms. The evaluated algorithms include our proposed SPR, PR, and CI, GND, FINDER, NEES, NIRM, DCRS, detailed definitions of the baseline dismantling algorithms are provided in the Baseline section. Results are shown for nine real-world networks: (a) Crime, (b) DNCEmails, (c) Figeys, (d) FilmTrust, (e) NetScience, (f) PPI, (g) RoviraVirgili, (h) KKI, and (i) EconPoli.

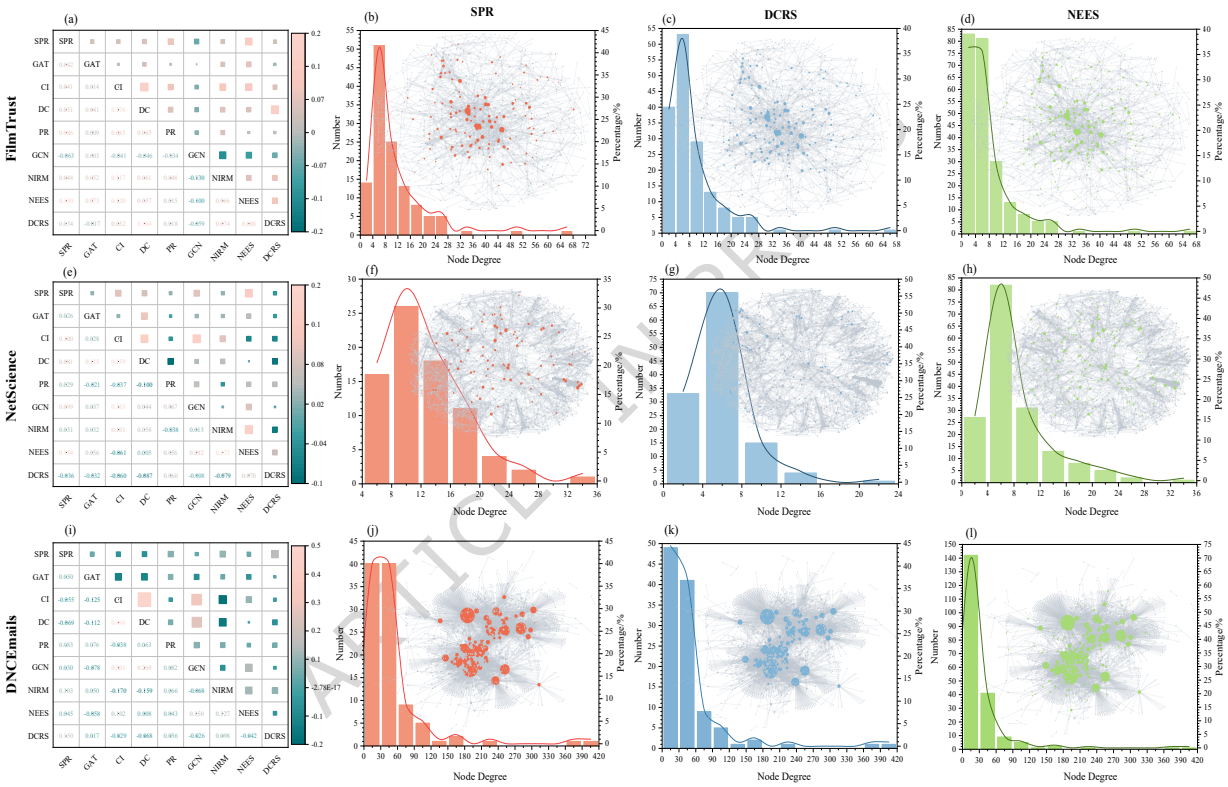


**Figure 3. Comparison of the node removal sequences generated by different methods.** The methods compared include SPR, GAT, CI, DC, PR, GCN, NIRM, NEES, DCRS, detailed definitions of the baseline dismantling algorithms are provided in the Baseline section. (a-d) FilmTrust Network; (e-h) NetScience Network; (i-l) DNCEmail Network. In FilmTrust Network, (a) show the Kendall correlation coefficients between the node removal sequences generated by different method. (b-d) visualizes the node degree distribution and attack nodes selected by SPR(red), DCRS(blue), and NEES(green) models. NetScience Network(e-h) and DNCEmail Network(i-l) are same as FilmTrust Network(a-d).

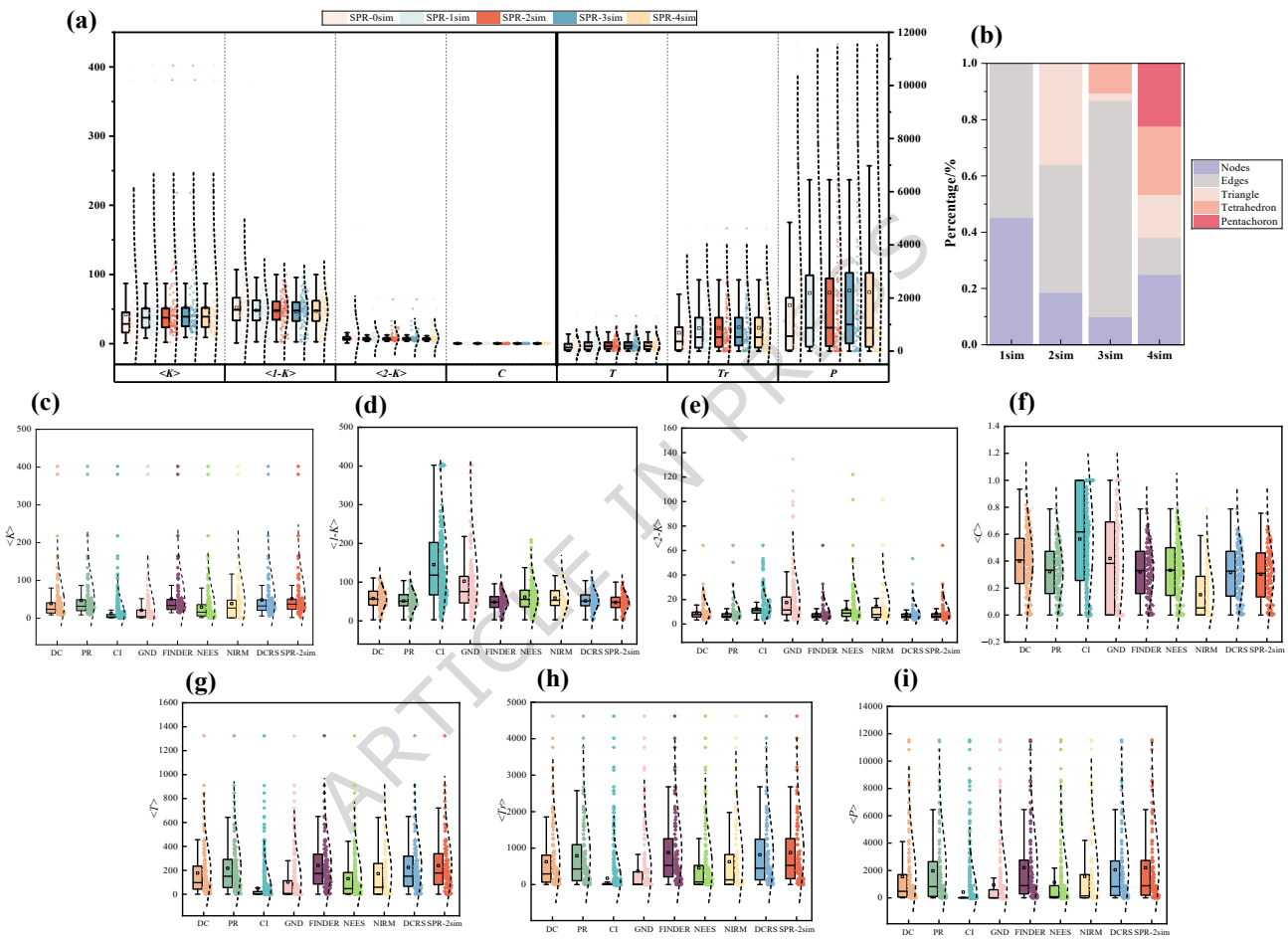


**Figure 4. Topological profile of the targeted attack node sets on the DNCEmails network.** The median and mean values in the box of (a), (c), (d), (e), (f), (g), (h) and (i) are represented by straight lines and squares, respectively. (a) Trends in topological properties of TAS identified by SPR as the aggregated simplex order $f$ increases from 0 to 4. (b) Contribution weights of each simplex order to the final node importance score. (c-i) Comparison between SPR-2sim and representative baselines in terms of topological characteristics of selected TAS: (c) node degree $< K >$, (d) average degree of 1-hop neighbors $< 1-K >$, (e) average degree of 2-hop neighbors $< 2-K >$, (f) local clustering coefficient $< C >$, (g) number of incident triangles $< T >$, (h) number of tetrahedra $< Tr >$, and (i) number of pentahedron $< P >$.

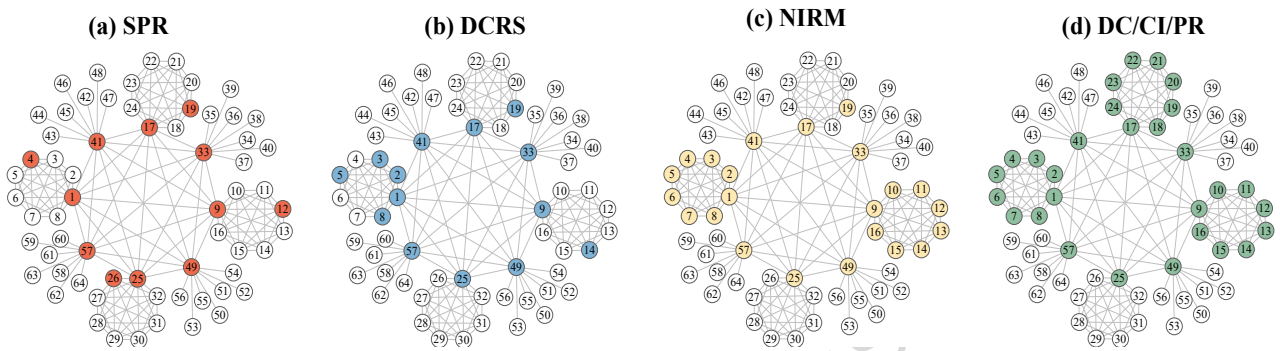


**Figure 5. Synthetic networks G of multiple cliques connected via hub nodes(the dismantling targets $\Theta_{GCC}$ = 0.1).** Different algorithms use different colors to distinguish the selected removal nodes, namely (a) SPR in red; (b) DCRS in blue; (c) NIRM in yellow; (d) DC/CI/PR in green. Detailed definitions of the baseline dismantling algorithms are provided in the Baseline section.



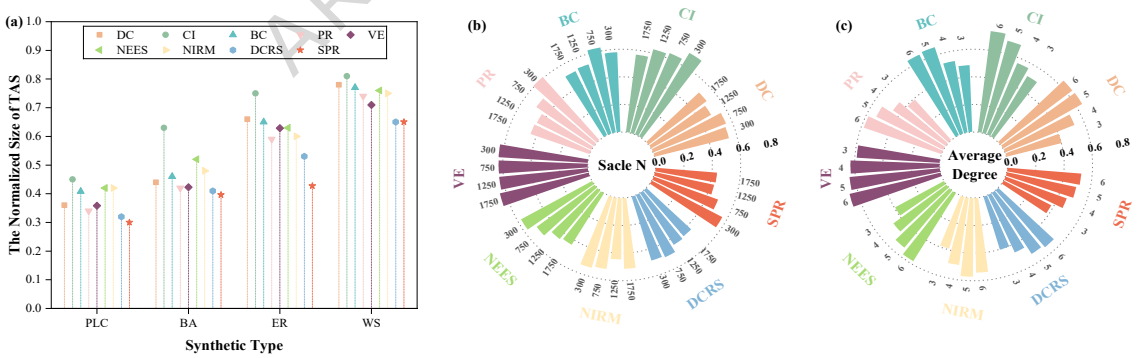


**Figure 6. Dismantling performance of SPR on synthetic model networks(the dismantling targets $\Theta_{GCC}$ = 0.01).** (a) The average performance of SPR in the dismantling of four synthetic networks. (b) the performance on ER networks with fixed network average degree $< k >= 4$ and varying network size $N$ from 100 to 2000. (c) the performance of normalized size of TAS on ER networks with fixed network size $N = 1000$ and varying $< k >$ from 3 to 6. Detailed definitions of the compared baseline dismantling algorithms are provided in the Baseline section.

**Table 1.** The performance of SPR in the dismantling of nine real-world networks (the dismantling targets $\Theta_{GCC} = 0.01$), the optimal dismantling costs is highlighted in **bold**, while the sub-optimal is in underline. Detailed definitions of the baseline dismantling algorithms are provided in the Baseline section.

| Baseline | FilmTrust | RoviraVirgili | DNCEmails | Figeys | PPI | NetScience | Crime | KKI | EconPoli |
|---|---|---|---|---|---|---|---|---|---|
| DC | 22.77 | 48.46 | 8.09 | 18.89 | 27.34 | 16.08 | 25.21 | 32.44 | 6.37 |
| BC | 33.75 | 54.55 | 15.7 | 18.89 | 35.70 | 30.05 | 36.79 | 24.71 | 14.95 |
| CC | 70.02 | 74.32 | 90.14 | 50.2 | 55.13 | 29.77 | 65.02 | 69.88 | 60.70 |
| EC | 89.93 | 79.88 | 90.25 | 56.90 | 60.52 | 98.29 | 75.51 | 74.71 | 68.31 |
| HC | 70.02 | 72.90 | 88.10 | 51.14 | 50.31 | 29.64 | 63.69 | 61.53 | 59.03 |
| PR | 22.20 | 44.40 | 6.16 | 16.03 | 24.19 | 19.71 | 27.26 | 22.03 | 5.99 |
| DR | 22.08 | 45.98 | 6.16 | 10.50 | 22.66 | 64.20 | 28.83 | 76.76 | 8.91 |
| CI | 42.68 | 59.31 | 30.33 | 25.90 | 34.67 | 28.95 | 42.82 | 50.58 | 5.64 |
| GND | **13.42** | 42.63 | 7.40 | 11.30 | 22.98 | 5.82 | 27.74 | 36.33 | 8.06 |
| VE | 29.63 | 52.43 | 15.43 | 20.05 | 36.33 | 17.73 | 48.13 | 40.30 | 5.89 |
| DW | 89.13 | 95.23 | 27.60 | 36.67 | 80.98 | 82.14 | 82.37 | 80.42 | 69.86 |
| NV | 64.87 | 94.88 | 31.62 | 86.02 | 41.32 | 68.45 | 91.54 | 84.89 | 62.37 |
| RV | 88.67 | 97.26 | 97.75 | 94.60 | 97.12 | 98.88 | 93.56 | 89.36 | 74.35 |
| GCN | 98.74 | 98.94 | 7.5 | 30.64 | 98.88 | 68.86 | 82.75 | 78.06 | 34.21 |
| GAT | 81.69 | 86.41 | 74.12 | 54.27 | 61.38 | 72.21 | 84.80 | 90.79 | 11.03 |
| FINDER | 16.82 | 41.65 | 5.52 | 11.75 | 27.29 | 11.57 | 25.09 | 20.20 | 63.55 |
| GDM | 14.87 | 42.36 | 5.79 | 9.30 | 22.48 | 6.84 | 25.33 | 18.77 | 5.96 |
| NIRM | 44.39 | 45.01 | 6.38 | 39.53 | 25.49 | 8.28 | 25.45 | 38.78 | 8.33 |
| NEES | 25.97 | 52.34 | 10.45 | 10.05 | 24.82 | 11.49 | 25.81 | 18.50 | 14.95 |
| DCRS | 19.11 | 43.07 | 5.89 | 8.93 | 21.67 | 8.42 | 26.06 | 22.34 | 6.58 |
| SPR | 14.30 | **40.86** | **5.36** | **8.71** | **21.31** | **5.75** | **23.88** | **16.26** | **4.99** |
| Improv.(%) | -2.31 | 1.90 | 2.90 | 2.46 | 1.66 | 1.20 | 4.82 | 12.11 | 11.52 |

**Table 2.** Ablation study of dismantling performance $\Theta_{GCC}$ when using node intermediate score and the final score.

| Methods | FilmTrust | RoviraVirgili | DNCEmails | Figeys | PPI | NetScience | Crime | KKI | EconPoli |
|---|---|---|---|---|---|---|---|---|---|
| w/o PR | 48.28 | 52.34 | 6.16 | 11.26 | 27.97 | 55.99 | 25.21 | 30.52 | 33.73 |
| w/o SR | 70.14 | 81.20 | 65.11 | 74.36 | 58.99 | 27.99 | 76.36 | 22.03 | 20.08 |
| SPR | **14.3** | **40.86** | **5.36** | **8.71** | **21.31** | **5.75** | **23.88** | **16.26** | **4.99** |

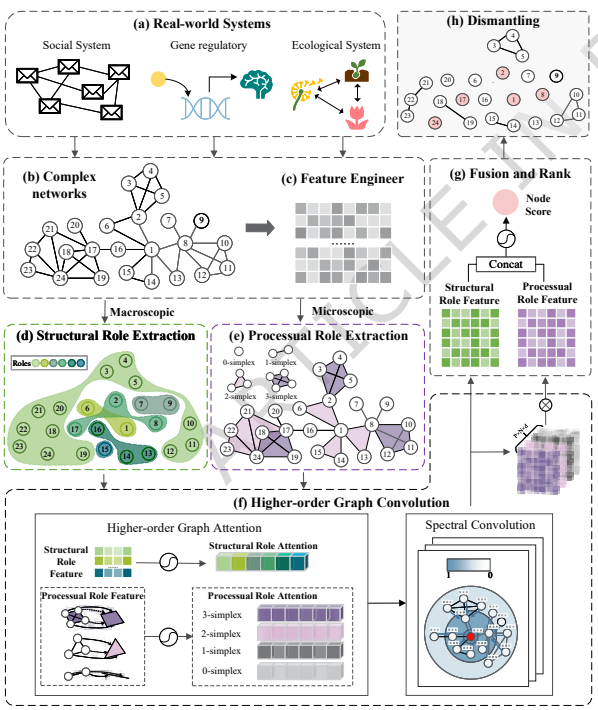

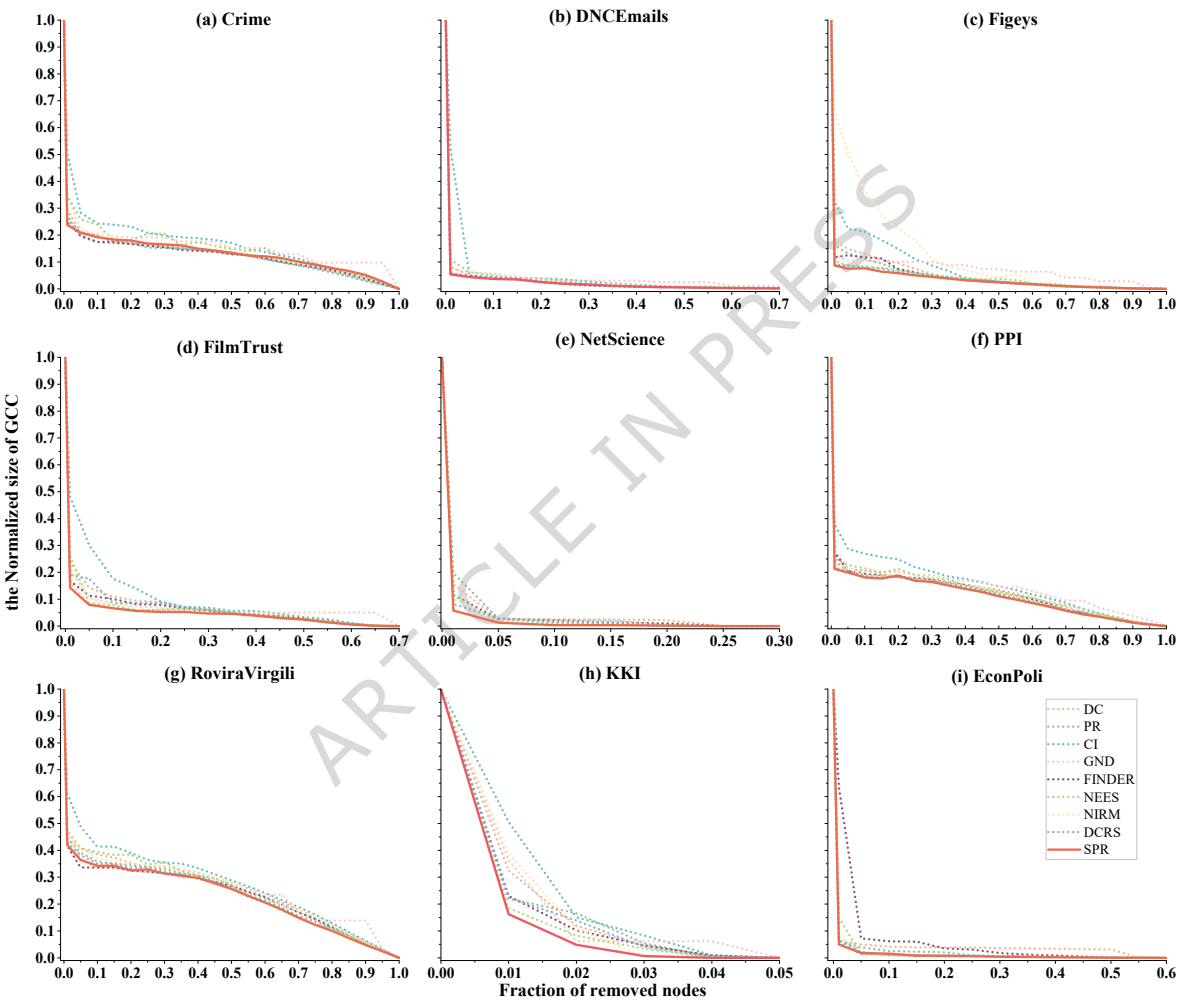

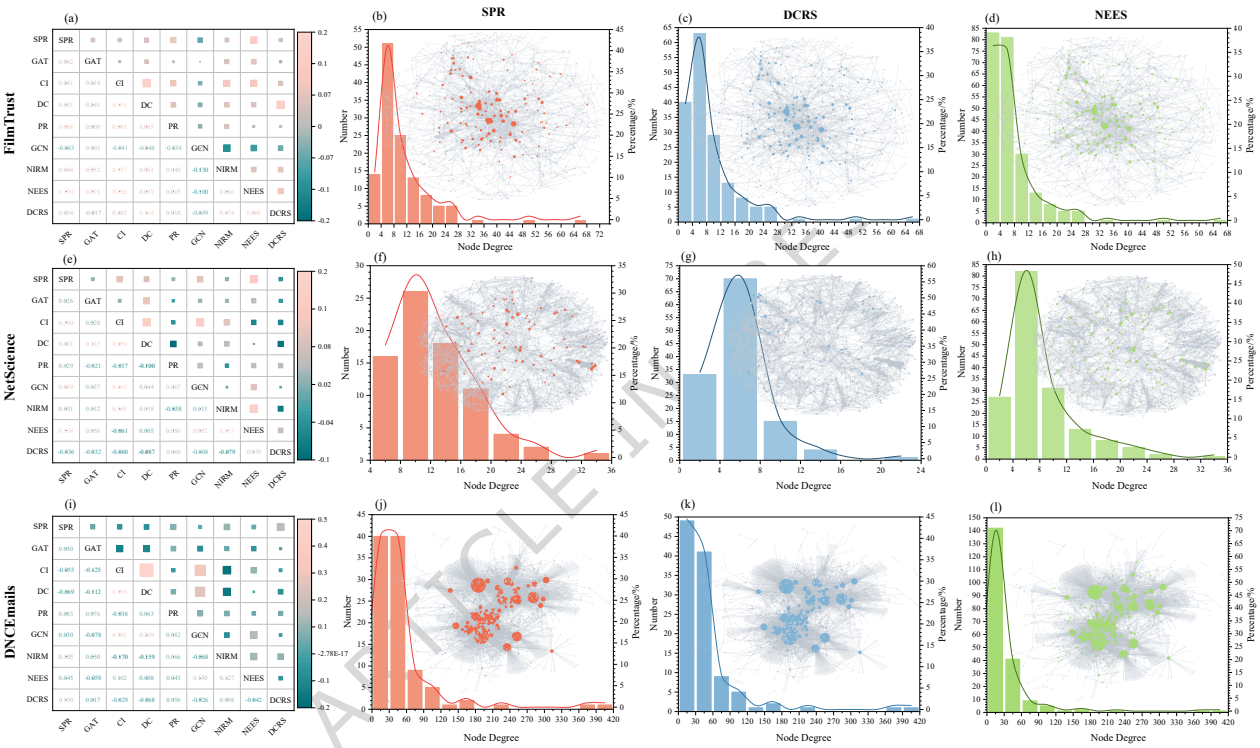

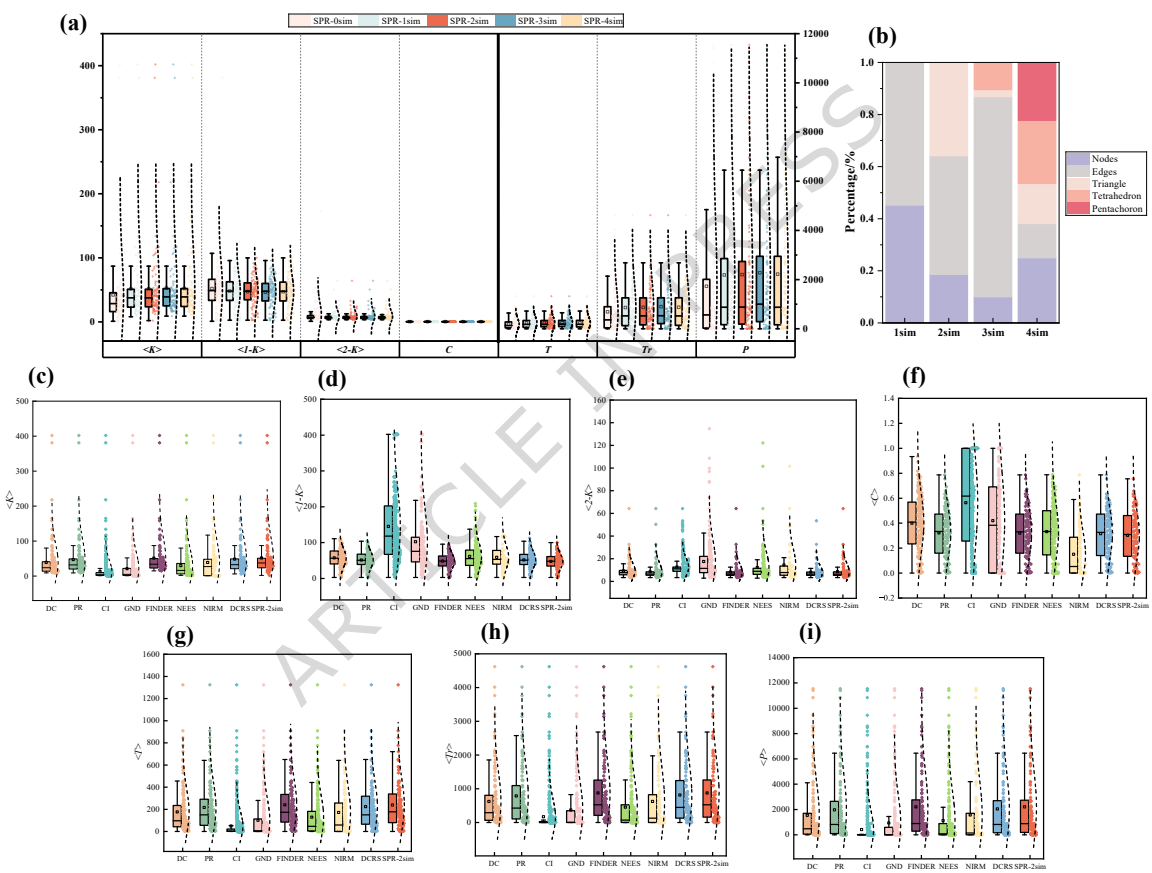

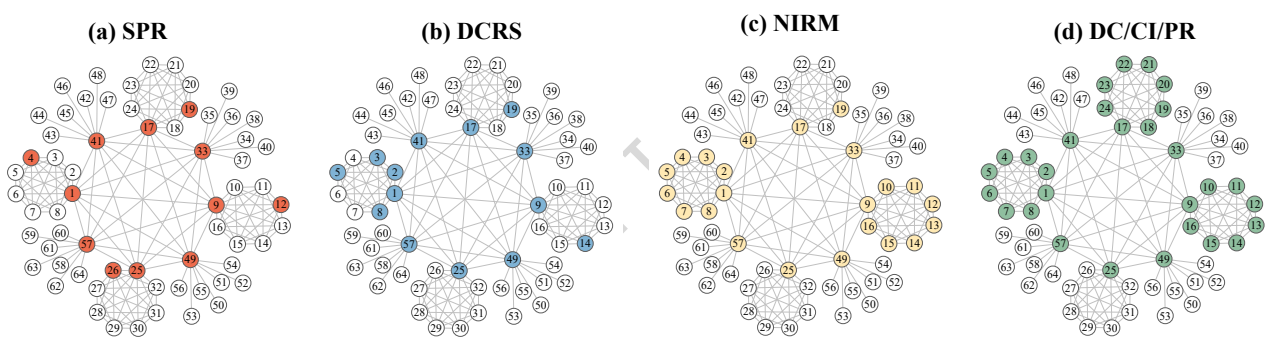
(a) SPR
(b) DCRS
(c) NIRM
(d) DC/CI/PR